Astron. Astrophys. 319, 981–994 (1997)

ASTRONOMY
AND
ASTROPHYSICS

Oscillations of the solar radial p-modes

Q.L. Cheng and D.R. Xiong

Purple Mountain Observatory, Academia Sinica Nanjing, 210008, P.R. China

Received 26 February 1996 / Accepted 3 June 1996

Abstract. We have calculated the radial non-adiabatic p-mode oscillations of the solar models. Based on a statistical theory of non-local convection, both the thermodynamic and kinetic couplings between convection and oscillations are finely treated. The turbulent pressure, turbulent viscosity, turbulent thermal flux and turbulent kinetic flux are all self-consistently included in the equations. The departure from the radiative equilibrium is treated exactly in the Eddington's approximation. The radiation field and gas are separately considered throughout, and they are coupled by the gaseous absorption and radiation. The generalized Mihalas' radiative hydrodynamic equations, and the dynamic equations of the auto- and the cross-correlations of the turbulent temperature and velocity fluctuations together form a set of self-consistent complete equations. It is shown by numeric calculation that all p-modes with n = 0 – 13 are pulsational unstable when the coupling between convection and oscillations was neglected, and the p-modes with n = 6 – 32 are unstable while that coupling was included. The thermodynamic coupling between convection and oscillations is the chief excitation mechanism, which occurs predominantly in the superadiabatic convection region. Turbulent pressure is always a destabilization factor. With increasing frequency, the turbulent viscosity increases more rapidly than the turbulent pressure does and becomes a dominate damping factor. The non-adiabatic effects on oscillation frequencies are not negligible, they caused a change of the frequencies up to several microhertzs. The departure from the radiative equilibrium has significant effects on stability of the solar p-modes. But these effects usually only alter the value of the stability coefficient but not its sign. The influence of the non-adiabatic effects and non-radiative equilibrium increases with increasing frequency of p-mode oscillations.

Key words: convection – Sun: oscillations; interior

1. Introduction

The stability of the solar p-mode oscillations has been studied by many authors (Ando & Osaki, 1975; Goldreich & Keeley, 1977; Antia, Chitre & Narasimha, 1982; Antia, Chitre & Gough, 1987; Gough, 1980; Christensen-Dalsgaard & Frandsen, 1983). The most thorough study was presented by Balmforth (1992). The results vary widely from one to another. It is mainly due to the different treatment of the coupling between convection and oscillations.

The convective envelope of the sun is very extended. It occupies the outmost layers of $0.3R_{\odot}$. The convective flux is more than 99.9% of total flux in the ionization zones of hydrogen and helium, where the κ mechanism should operate. Thus, convection is the main factor which affects the stability of the solar p-mode oscillations. The results differ seriously with different treatments of convection (Gough 1980; Antia et al. 1982; Balmforth 1992).

To investigate the coupling between convection and pulsation, we have developed a time-dependent convection theory (Xiong, 1977, 1989). The later is a non-local statistical theory of time-dependent convection. The turbulent pressure is included self-consistently in the radiative hydrodynamic equations. So it can be used to study both thermodynamic and dynamic couplings between convection and pulsation. Our theory is deduced strictly from the hydrodynamic equations and the theory of turbulence. It can be used for a more correct description of the dynamic behavior of turbulent convection and a more accurate treatment of the coupling between pulsation and convection. We will list the basic equations for numeric computation in Sect. 2. the numerical results and a brief analysis and discussion are given in Sect. 3. Finally, some conclusions and discussion are drawn in Sect. 4.

2. Equations of radial non-adiabatic oscillations of stars

The basic equations for calculations in this paper is the radiative-hydrodynamic equations developed by one of the authors (Xiong, 1989) with the following inprovements:

1). The departure from radiative equilibrium has been considered in detail throughout the deducing of the equations. The gas and radiation field have been described completely separately, and they are coupled through the emission and absorbtion by gas.

2). The non-isotropic component of the turbulent Reynolds stress, therefore the turbulent viscosity, has been included.

As a whole, the pulsational equations consist of 11 first-order linear differential equations: the first five are dynamic equations describing the motion of the fluid and the radiation field, and the last six are dynamic equations describing convection. All equations and the boundary conditions are given in the Appendix.

3. Numeric results

3.1. Equilibrium model

Removing in the equations of the Appendix the terms with u and the derivatives with respect to t, which are equal to zero for the steady stellar models, it is not difficult to obtain the equations of equilibrium model.

Here we should point out that, the effects of non-radiative equilibrium have been considered strictly (in the frame of Eddington approximation) in our calculation of the equilibrium envelope model. Usually, one calculates stellar envelope models by a simple integration from the stellar surface to its interior. This is an initial value problem of ordinary differential equations of order 3. But our problem, considering the effects of non-radiative equilibrium and using a non-local convection theory, becomes a boundary problem of 10 ordinary equations. This brings us much complexity and more difficulties in numerical treatment.

The calculation of the solar envelope equilibrium model is very similar to that described in our previous paper (Xiong & Cheng, 1992). The only changes are, as declared in Sect 2: the solar mass $M_\odot$ = $1.989 \times 10^{33} g$, luminosity $L_\odot$ = $3.826 \times 10^{33} ergs/s$, chemical composition (X, Z) = $(0.70, 0.02)$, and the two convection parameters (c_1, c_2) = $(0.75, 0.75)$, which is, according to the convective energy transport efficiency, correspond to the case of the original mixing length theory with a mixing length equal to 1.5 times the pressure scale height. In our computation of the equilibrium envelope model, the lower boundary model is placed at the temperature $T_b \approx 7.8 \times 10^6 K$, where $r = r_b$ = $0.27 R_\odot$. The surface boundary is at the optical depth τ = 10^{-4}.

At first sight, the dynamic equations of turbulent convection (A10) – (A15) are very different from those used in our earlier papers (Xiong, 1989; Xiong & Cheng, 1992). These differences are due to the different treatment of the radiation fields. In the present paper the gas and the radiation fields are treated separately and they couple each other through the emission and absorption of the gas (refer to Eqs. (A7) and (A8)). All the state parameters and thermodynamic variables (e.g. A, B, C_p, ∇_{ad},...) are the material properties without the contribution of the radiation fields. We have proved that the new dynamic equations (A10) – (A15) are consistent with the earlier ones (Xiong, 1994). This is confirmed by the numerical calculations. The equilibrium model here is very close to model 1 in our earlier paper (Xiong & Cheng 1992). The slight differences between them comes mainly from the different equations of state and the different values of diffusion parameter c_2 used. The most remarkable characteristics of our model differing from other models using a non-local mixing-length theory are the following facts: 1) our model has a rather steep temperature gradient in the solar atmosphere, which is consistent with observations. 2) there is a "super-radiative temperature gradient" ($\nabla > \nabla_{rad}$) in the lower convective overshooting zone adjacent to the local convective unstable zone, because the convective flux will become negative there as predicated by our theory. The maximum magnitude of the negative convective flux is about ten percent of the total flux. The temperature and radius at the bottom boundary of the local convective unstable zone are about $T \sim 1.7 \times 10^6 K$ and $r \sim 0.7 R_\odot$ respectively. The general characteristics of the equilibrium model can be found in our earlier paper (Xiong & Cheng 1992).

We use a simplified MHD equation of state (Hummer & Mihalas 1988, Mihalas et al 1988, Däppen et al 1988) in our present work. Neutral helium is considered as hydrogen-like atom. In fact, when helium atoms are in higher excited states, their behaviour is very similar to hydrogen. Significant departure only appears when they are in the ground and lower excited states. We think this simplification introduces minor errors but is very convenient when calculating the equation of state.

3.2. Calculation of non-adiabatic pulsation

To investigate the influence of radiation and convection on solar p-mode oscillations, we calculated two series of solar linear non-adiabatic pulsations:

1). Neglecting the coupling between convection and pulsation. Assuming convection does not vary during pulsations, Eqs. (A49) - (A54), which are describing the pulsational variation of convection, can be omitted, and the terms with convective variables in Eqs.(A44) - (A48) can also be omitted. After doing so, the order of pulsation equations is reduced to 5, and the convective variables disappear from the equations. (Notice: of course convection is still included in the equilibrium model !!).

2). The coupling is included. The linear non-adiabatic pulsation equations are consist of 11 linear ordinary equations : Eqs. (A44) - (A54). The surface boundary condition are set at τ = 10^{-4}.

The numerical results of solar radial non-adiabatic p-mode oscillations with n=0 – 34 are presented in Table 1. The first column are the radial order n, the second are ν_{ad}, the frequencies of adiabatic oscillation. The third and fourth columns are $\nu - \nu_{ad}$, the differences between the frequencies of adiabatic and non-adiabatic pulsation, and $-\omega_i$, the amplitude growth rates for case 1 (without convective coupling). The fifth and sixth columns are the same as the third and fourth, but for case 2 (with the convective coupling).

3.2.1. Pulsational stability of solar radial p-modes

When coupling between convection and pulsation is not considered, all the solar radial modes with $n > 13$ are stable. This differs much from the results by Ando & Osaki (1975). This may be due to a different treatment of the upper atmosphere of the Sun. Ando and Osaki adopted the solar atmosphere temperatures from the Harvard-Smithsonian Reference Atmosphere, which is not consistent with the equation of radiation transfer

Table 1. Frequency difference and amplitude growth rate for solar p-modes

C_1 = 0.75 C_2 = 0.75 τ = 4.0 × 10^{-04}

		radiative Eddington appromaxion				radiative diffusion appromaxion			
		without conv.		with conv.		without conv.		with conv.	
n	ν_{ad}	$\nu_r - \nu_{ad}$	rate	$\nu_c - \nu_{ad}$	rate	$\nu_r - \nu_{ad}$	rate	$\nu_c - \nu_{ad}$	rate
0	257.64	-1.01	1.1E-13	-1.01	-1.2E-11	-1.01	1.1E-13	-1.01	-1.8E-11
1	428.89	-0.84	7.2E-13	-0.84	-2.8E-11	-0.84	7.4E-13	-0.84	-4.3E-11
2	588.20	-0.88	4.5E-12	-0.87	-1.9E-10	-0.88	4.7E-12	-0.88	-2.8E-10
3	750.99	-0.91	2.4E-11	-0.91	1.8E-10	-0.91	2.5E-11	-0.91	-1.1E-09
4	911.62	-0.97	9.6E-11	-0.96	4.2E-10	-0.97	1.1E-10	-0.96	-1.7E-09
5	1068.76	-1.07	3.2E-10	-1.05	-3.6E-10	-1.07	3.7E-10	-1.05	2.9E-10
6	1226.95	-1.16	9.2E-10	-1.12	1.6E-09	-1.16	1.1E-09	-1.12	1.0E-08
7	1385.35	-1.26	2.5E-09	-1.17	1.8E-08	-1.26	3.2E-09	-1.16	-1.5E-08
8	1540.21	-1.34	6.4E-09	-1.15	6.4E-08	-1.34	9.0E-09	-1.14	5.4E-08
9	1690.78	-1.41	1.4E-08	-1.03	1.4E-07	-1.41	2.2E-08	-0.99	1.2E-07
10	1839.27	-1.51	2.5E-08	-0.86	3.5E-07	-1.52	4.6E-08	-0.79	3.8E-07
11	1988.30	-1.66	3.4E-08	-0.65	7.8E-07	-1.67	7.9E-08	-0.56	7.3E-07
12	2138.14	-1.81	3.4E-08	-0.34	1.4E-06	-1.83	1.3E-07	-0.16	1.2E-06
13	2287.60	-1.97	8.3E-09	0.17	2.7E-06	-2.01	1.9E-07	0.47	2.3E-06
14	2435.91	-2.18	-7.7E-08	0.80	4.2E-06	-2.26	2.5E-07	1.24	3.9E-06
15	2583.95	-2.44	-2.5E-07	1.50	6.7E-06	-2.58	2.8E-07	1.62	6.4E-06
16	2733.11	-2.74	-5.5E-07	1.88	8.6E-06	-2.95	2.4E-07	2.42	8.0E-06
17	2883.55	-3.09	-1.0E-06	2.30	1.2E-05	-3.39	1.1E-07	2.67	1.0E-05
18	3034.64	-3.47	-1.7E-06	2.92	1.5E-05	-3.92	-1.5E-07	2.70	1.2E-05
19	3186.26	-3.90	-2.6E-06	3.35	1.7E-05	-4.53	-5.7E-07	2.56	1.3E-05
20	3338.47	-4.37	-3.8E-06	3.59	2.1E-05	-5.24	-1.2E-06	2.60	1.5E-05
21	3491.14	-4.87	-5.2E-06	3.45	2.4E-05	-6.03	-2.1E-06	2.70	1.8E-05
22	3644.34	-5.40	-7.0E-06	3.24	2.6E-05	-6.92	-3.2E-06	2.31	2.3E-05
23	3798.24	-5.95	-9.2E-06	3.10	2.6E-05	-7.91	-4.7E-06	1.41	3.5E-05
24	3952.70	-6.53	-1.2E-05	2.99	3.1E-05	-9.01	-6.6E-06	0.98	7.3E-06
25	4107.62	-7.13	-1.5E-05	2.22	2.9E-05	-10.25	-9.0E-06	-1.69	3.0E-05
26	4263.10	-7.77	-1.8E-05	1.92	3.2E-05	-11.70	-1.2E-05	1.71	-8.1E-06
27	4418.99	-8.46	-2.3E-05	1.01	2.7E-05	-13.38	-1.6E-05	-7.95	5.1E-05
28	4575.05	-9.18	-2.7E-05	0.04	2.7E-05	-15.32	-2.1E-05	-4.63	2.9E-06
29	4731.38	-9.92	-3.3E-05	-0.11	2.5E-05	-17.55	-2.6E-05	6.65	5.3E-05
30	4888.09	-10.68	-4.0E-05	-1.31	1.7E-05	-20.10	-3.3E-05	-13.51	9.9E-05
31	5045.05	-11.46	-4.7E-05	-2.36	1.2E-05	-23.05	-4.1E-05	-21.72	-3.8E-05
32	5202.29	-12.26	-5.6E-05	-3.84	5.8E-06	-26.51	-5.1E-05	-19.12	-4.6E-05
33	5359.87	-13.10	-6.6E-05	-5.20	-3.4E-06	-30.62	-6.1E-05	-20.63	-5.7E-05
34	5517.66	-13.98	-7.7E-05	-6.45	-1.4E-05	-35.46	-7.3E-05	-24.26	-7.8E-05

(A9). The error in equilibrium model will be brought into the linear oscillation equation (A48). We calculated such a solar envelope model: Placing the surface boundary at the optical depth $\tau = 0.2$, where the gaseous pressure, temperature and radius are taken from Harvard-Smithsonian Reference Atmosphere (Gingerich, et al., 1971), the structure of the solar convective envelope is calculated using our non-local convection scheme. The temperature-pressure structure above $\tau = 0.2$ up to the temperature minimum are directly taken from Harvard-Smithsonian Reference Atmosphere. We applied the same linear non-adiabatic oscillation equations described in previous section to this mixed envelope model, and got the result that all the solar radial p-modes with $n \leq 29$ are unstable when the coupling between convection and pulsation being omitted. This, to some extent, proved our guess.

When the coupling between convection and pulsation is considered, all the solar radial modes with $6 \leq n \leq 32$ are pulsationally unstable. The variations of the amplitude growth rate with frequencies of oscillations are shown in Fig. 1. The amplitude growth rate achieves its maximum near $\nu \approx 4000\mu H_z$. It decreases rapidly and becomes negative towards higher frequency end. In the intermediate and low frequency region,

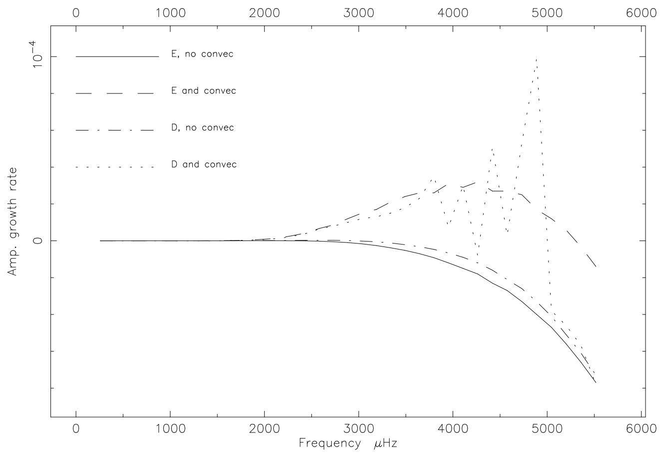

Fig. 1. The amplitude growth rate, η *vs* frequency for the solar radial p-modes. The dashed and solid lines are for the Eddington approximation with and without convective coupling respectively. The dotted and dash-dotted lines are for the radiative diffusion approximation.

($4000 > \nu > 1500\mu H_z$), it runs fairly smoothly. When frequency becomes lower further, it falls down quickly and finally changes sign.

Eq. (A45) can be rewritten as

$$\begin{aligned}4\pi r^3 & \tfrac{d}{dM_r}(\delta P_g + \delta P_t + \delta P_r) \\ & - \tfrac{16\pi}{3}\tfrac{d}{dM_r}\{[GM_r\rho rBV\tau_c^* + \tfrac{i\omega\tau_c^*}{1+i\omega\tau_c^*}(\rho r^3 x^2 \\ & + \tfrac{4}{3}GM_r\rho rBV\tau_c^*)]\tfrac{dy_3}{d\ln r} \\ & + \tfrac{GM_r\rho rBV\tau_c^*}{1+i\omega\tau_c^*}[(2 + \tfrac{r^3\omega^2}{GM_r} + 2i\omega\tau_c^*)y_3 - y_{10}]\} \\ & - [4\tfrac{d}{dM_r}(GM_r\rho rBV\tau_c^*) + \tfrac{GM_r}{r} + r^2\omega^2]y_3 = 0,\end{aligned} \tag{1}$$

where $P_r = E_r/3$ and $P_t = \rho x^2$ are the radiation and the turbulent pressures respectively. Following Backer and Gough (1979, it is not difficult to get the linear stability coefficient η from Eq. (1),

$$\eta = -\frac{2\pi\omega_i}{\omega_r}$$

$$= F + W_{P_r}(M_0) + W_{P_g}(M_0) + W_{P_t}(M_0) + W_{vis}(M_0), \tag{2}$$

where W_{P_r}, W_{P_g}, W_{P_t} and W_{vis} are the normalized accumulated works done by the radiation pressure, the gas pressure, the turbulent pressure and the turbulent viscosity respectively,

$$W_{P_r}(M) = -\frac{1}{2E_k}\int_{M_b}^{M}\frac{1}{\rho^2}I_m(\delta P_r\delta\rho^*)dM_r, \tag{3}$$

$$W_{P_g}(M) = -\frac{1}{2E_k}\int_{M_b}^{M}\frac{1}{\rho^2}I_m(\delta P_g\delta\rho^*)dM_r, \tag{4}$$

$$W_{P_t}(M) = -\frac{1}{2E_k}\int_{M_b}^{M}I_m\{\frac{1}{\rho^2}\delta P_t\delta\rho^*$$

$$+\frac{2}{3}\frac{BVr\omega^2\tau_c^*}{1+i\omega\tau_c^*}(\frac{r^3\omega^2}{GM_r}y_3 - y_{10})\frac{dy_3^*}{d\ln r}\}dM_r, \tag{5}$$

$$W_{vis}(M) = -\frac{2}{3E_k}\int_{M_b}^{M}\frac{\omega_r\tau_c^*}{1+i\omega_r^2\tau_c^*}(x^2$$

$$+\frac{4}{3}\frac{GM_r}{r^2}BV\tau_c^*)\frac{dy_3}{d\ln r}\frac{dy_3^*}{d\ln r}dM_r, \tag{6}$$

where M_b is the mass interior the base of the envelope and E_k is the whole kinetic energy of oscillations,

$$E_k = \frac{1}{2}\omega_r^2\int_{M_b}^{M}r^2 y_3 y_3^* dM_r = \frac{1}{2}\omega_r^2\int_{M_b}^{M}\delta\boldsymbol{r}\cdot\delta\boldsymbol{r}^* dM_r, \tag{7}$$

and

$$\begin{aligned}F = & \tfrac{2\pi}{E_k}I_m\{[\tfrac{4}{3}\tfrac{\omega_r\tau_c^*}{1+i\omega_r^2\tau_c^*}(\rho r^3x^2 + \tfrac{4}{3}GM_r\rho rBV\tau_c^*)\tfrac{dy_3}{d\ln r} \\ & \tfrac{4}{3}\tfrac{GM_r\rho rBV\tau_c^*}{1+i\omega\tau_c^*}(\tfrac{r^3\omega^2}{GM_r}y_3 - y_{10}) \\ & - r^3(\delta P_g + \delta P_t + \delta P_r)]y_3\}_{M=M_0}.\end{aligned} \tag{8}$$

If the surface boundary is set at the upper layer of atmosphere optical thin enough, F will be far smaller than W_{P_g}, therefore it will be negligible.

$W_{all} = \Sigma W_i$, $W_{P_r}(M_0)$, $W_{P_g}(M_0)$, $W_{P_t}(M_0)$ and $W_{vis}(M_0)$ for n = 0–34 p-modes are listed in Tables 2 and plotted in Fig. 2. The linear stability coefficient, $\eta_i = -2\pi\omega_i/\omega_r$ given by pulsational calculations, in general, agree well with W_{all} given by the work integeral.

W_{all}, W_{P_r}, W_{P_g}, W_{P_t} and W_{vis} are plotted as functions of $logP_g$ in Fig. 3 for the 21st order overtone mode. We can see that:

1) W_{P_r} is much smaller than W_{P_g}, W_{P_t} and W_{vis} for the Sun. It is true for the Sun-like stars.

2) W_{vis} is always negative, because the turbulent viscosity transforms the kinetic energy of oscillations into thermal energy. Therefore, it damps the stellar oscillations. $|W_{vis}|$ increases rapidly with the increasing of frequency. and become much larger than W_{P_t} in the frequency band of the solar 5-min oscillations. It is due to that the velocity gradient increases rapidly with the radial order n.

3) W_{P_t} is positive for most modes. We argued that the variation of turbulent pressure, in general, lags behind the variation of the gas density, at least in the local time-dependent theory of convection (Xiong, 1977). $(\delta P_t, -\delta\rho/\rho^2)$ will form a clockwise cycle in the P_t-V work diagram during the oscillation of star, namely the turbulent kinetic energy will be transformed into pulsational energy.

The sum of W_{P_t} and W_{vis} is the effect of the so-called dynamic coupling between convection and oscillations. Except for the fundamental mode (and possible for few low order modes also), $|W_{vis}|$ is much larger the W_{P_t}. Hence, the dynamic coupling between convection and oscillations plays a damping effect on the solar 5-min oscillations.

4) When the coupling between convection and oscillations is taken into account, W_{P_g} increases by few order of magnitude in comparison with the results without coupling. This is not difficult to understand. The ratio of the convective flux to the radiative one $L_c/L_r \sim 10^3$–10^6 in the ionized regions of hydrogen and helium, where the κ-mechanism operates. The

Table 2. Amplitude growth rate, work integral and its components

			C_1 = 0.75	C_2 = 0.75	τ = 4.0 × 10^{-04}		
n	ν	η	W_{all}	W_{pr}	W_{pg}	W_{pt}	W_{vis}
0	257	-4.780E-08	-5.083E-08	-2.543E-10	-1.333E-07	1.040E-07	-2.132E-08
1	428	-6.524E-08	-6.480E-08	-1.358E-10	5.331E-07	-3.348E-09	-5.945E-07
2	587	-3.176E-07	-3.185E-07	1.281E-10	4.743E-06	-3.056E-06	-2.005E-06
3	750	2.426E-07	3.088E-07	6.716E-10	2.037E-05	4.692E-07	-2.054E-05
4	910	4.569E-07	6.700E-07	1.348E-09	1.110E-04	1.953E-06	-1.123E-04
5	1068	-3.359E-07	-3.042E-07	-2.389E-09	3.474E-04	6.195E-06	-3.539E-04
6	1226	1.269E-06	9.087E-07	-3.284E-09	9.899E-04	1.167E-05	-1.001E-03
7	1384	1.314E-05	1.398E-05	7.797E-09	1.727E-03	2.475E-05	-1.738E-03
8	1539	4.164E-05	3.854E-05	1.096E-08	5.648E-03	4.162E-05	-5.651E-03
9	1689	8.302E-05	8.511E-05	-8.464E-09	1.591E-02	1.488E-04	-1.597E-02
10	1838	1.891E-04	1.938E-04	-1.184E-10	3.359E-02	2.376E-04	-3.363E-02
11	1987	3.905E-04	3.775E-04	2.814E-08	2.563E-02	7.704E-05	-2.533E-02
12	2136	6.765E-04	6.685E-04	1.887E-07	8.003E-02	5.416E-04	-7.991E-02
13	2286	1.167E-03	1.163E-03	4.005E-08	1.268E-01	5.869E-04	-1.262E-01
14	2434	1.720E-03	1.709E-03	5.249E-07	1.361E-01	7.246E-04	-1.352E-01
15	2582	2.608E-03	2.560E-03	7.971E-07	3.679E-02	-7.182E-04	-3.351E-02
16	2730	3.134E-03	3.088E-03	3.299E-07	1.903E-01	1.109E-03	-1.883E-01
17	2880	4.202E-03	4.153E-03	2.975E-07	3.382E-01	1.274E-03	-3.353E-01
18	3031	4.857E-03	4.801E-03	5.907E-07	2.702E-01	-8.054E-04	-2.645E-01
19	3182	5.431E-03	5.339E-03	1.111E-06	2.051E-01	-1.446E-03	-1.983E-01
20	3334	6.136E-03	6.048E-03	6.184E-07	5.508E-01	-6.997E-04	-5.441E-01
21	3486	6.995E-03	6.867E-03	-1.332E-07	1.172E+00	3.472E-03	-1.168E+00
22	3639	6.998E-03	6.853E-03	6.085E-07	7.066E-01	3.654E-03	-7.035E-01
23	3792	6.879E-03	6.729E-03	1.875E-06	1.662E-01	1.381E-03	-1.608E-01
24	3946	7.763E-03	7.618E-03	2.459E-06	2.975E+00	1.020E-02	-2.978E+00
25	4100	6.963E-03	6.818E-03	1.477E-06	6.801E-01	3.806E-03	-6.770E-01
26	4255	7.387E-03	7.252E-03	-4.298E-06	4.791E+00	1.061E-02	-4.795E+00
27	4411	6.127E-03	5.986E-03	2.059E-06	7.713E-01	2.896E-03	-7.682E-01
28	4566	5.794E-03	5.664E-03	2.084E-07	2.562E+00	9.767E-03	-2.566E+00
29	4721	5.345E-03	5.261E-03	-7.069E-06	6.604E+00	1.174E-02	-6.610E+00
30	4877	3.385E-03	3.328E-03	2.376E-06	1.685E+00	4.611E-03	-1.686E+00
31	5034	2.397E-03	2.355E-03	-4.457E-07	2.273E+00	7.301E-03	-2.278E+00
32	5190	1.121E-03	1.119E-03	-5.030E-07	3.477E+00	1.044E-02	-3.486E+00
33	5347	-6.397E-04	-5.628E-04	-2.545E-06	4.984E+00	1.553E-02	-5.000E+00
34	5504	-2.603E-03	-2.440E-03	-4.610E-06	6.773E+00	1.824E-02	-6.794E+00

convective flux will modulate more effectively the energy flux than the radiative flux does. The convective flux plays a dominate role in the modulation of gas pressure. The thermodynamic excitation of oscillations attributed to the convective flux occurs predominantly in the superadiabatic convection region, where the convective flux decreases rapidly and the convective inertia time-scale τ_c is near the minimum. This region will trap more thermal energy when it is more denser and hotter. Therefore, the behavior of this region is very similar to a thermal machine: namely, it transforms the thermal energy into kinetic energy of oscillations. This means that the thermodynamic coupling between convection and oscillations has a destabilizing effect on p-mode oscillations, at least for the solar 5-min oscillations. In fact, W_{P_g} includes the contribution of both the radiative and convective fluxes. It is difficult to separate them.

Our results are very different from those of Balmforth:

1) All the radial p-modes are stable in Balmforth's calculations, but the modes with order of 5th – 32nd are unstable in our results.

2) The absolute values of our linear stability coefficients are one order of magnitude larger than Balmforth's ones (1992a).

Obviously, the different treatment of convection is the most important cause. Balmforth used a modified Spiegel (1963) and Gough (1976) non-local mixing-length formulations. In

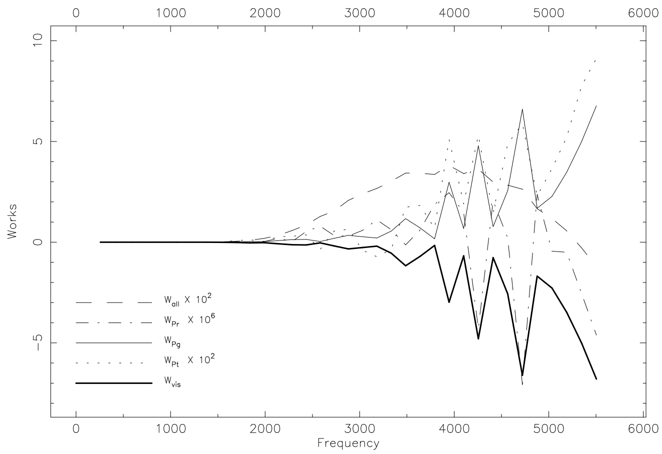

Fig. 2. The work integral W_{all} (dashed line) and its components W_{P_r} (dash dotted), contributed by radiative pressure, W_{P_g} (solid) by gaseous pressure, W_{P_t} (dotted) by turbulent pressure, and W_{vis} (thick solid) by viscosity, *vs* frequency.

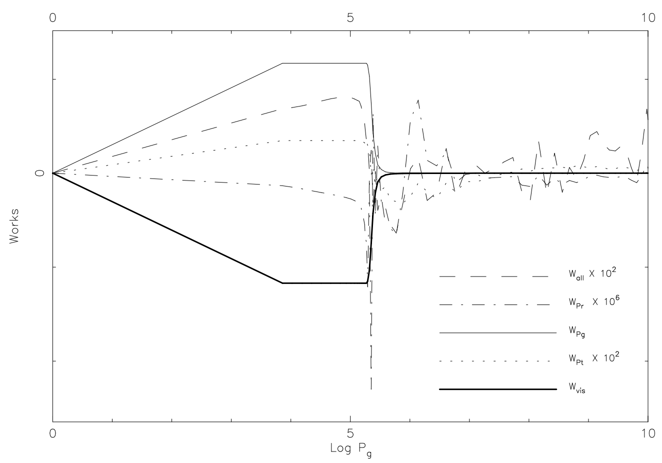

Fig. 3. The work integral and its components. *vs* log P_g for the 21st overtone of the solar radial p-mode. Other notations are the same as in Fig. 2.

the present paper we used a statistical theory of non-local time-dependent convection. It is derived from the radiation-hydrodynamic equations and turbulent theory (Xiong, 1989), therefore it should have sounder hydrodynamic basis than the usual mixing-length theory. Balmforth and Gough (1988) compared the result of calculation of RR Lyrae using Gough's local time-dependent mixing-length theory with the one using Xiong's local time-dependent statistical theory. They found that these two results are comparable. Non-local convection is more complex than local convection. The convective flux predicted by Spiegel's non-local mixing-length theory is positive in the overshooting region, so the theoretical temperature gradient of the solar atmosphere given by his theory is too gentle (Travis & Matsushima, 1973). Ulrich's theory is similar to Spiegel's. Differing from Spiegel's theory, according to our non-local theory of convection, the convective flux changes its sign when passing through the boundary of the local convective unstable zone. The convective flux is negative in the overshooting zone. Our theory predicts a larger temperature gradient in the solar atmosphere and a super-radiative temperature gradient in the bottom overshooting zone. Shown by our numerical tests. the non-local convective effects have significant influence on the stability of p-modes. The amplitude growth rates of seven solar envelope models with different convective diffusion parameter c_2 are listed in Table 3. There are two convective parameters c_1 and c_2 in our non-local convection theory. c_1 determines the efficiency of convective transport of energy, therefore determines the deepness of the solar convection zone. $c_2 H_p$ is the convective diffusion length, where H_p is the local pressure scale height. The overshooting distance (the e-folding length of turbulent velocity) is about $1.4\sqrt{c_1 c_2} H_p$ (Xiong & Cheng, 1992). Putting c_2 = 0, our non-local theory will return to the local one. Therefore, it can be used to investigate the influence of non-local convective effects on the stability by changing c_2. It is reasonable to believe that $c_1 \approx c_2$ (Xiong et al, 1995) in reality.

The numerical tests show that the influence of the upper atmosphere on the stability is not negligible, especially for the high order p-modes. It may be another important cause leading to the differences between Balmforth's results and ours. The amplitude growth rates for the same model (c_1 = c_2 = 0.75), but with the surface boundary set at τ = 10^{-4} are listed in the 2nd column of Table 3.

3.2.2. The influence of non-adiabatic effects on frequencies of solar p-mode oscillations

AS shown by numerical results, the non-adiabatic effects exert a non-negligible influence on the frequencies of the solar p-mode oscillations. The variations of frequency, $\Delta\nu$, caused by the non-adiabatic effects are about several microhertzs. The differences of frequency between the non-adiabatic and adiabatic oscillations are plotted vs frequency in Fig. 4. For the case omitting the coupling between convection and oscillations the curves descend monotonicaly with the increasing of frequency (except the fundamental mode). When the coupling is considered the curves have maxima near $3400\mu H_z$. Towards both lower and higher frequency ends, the frequencies of non-adiabatic oscillations, relative to the adiabatic ones, are systematically decreasing. Compared with Balmforth's (1992) results, there are two remarkable differences:

a). In Balmforth's calculation, the frequencies of non-adiabatic oscillations are systematically higher than those of the adiabatic ones, while our results are the reverse: the frequencies of non-adiabatic oscillations are systematically lower than adiabatic ones for the low- and high-order modes.

b). In magnitude, our predicted relative variations of frequency are larger than those of Balmforth.

Because of possible numerical errors, the influence of non-adiabatic effects on the frequencies of the p-mode oscillations must be carefully studied. For adiabatic case, Eqs. (A49) - (A54), which describe the time-dependent convection and the equation

Table 3. Work integral for different convective parameter C_2

n	0.750	0.750	0.500	0.375	0.250	0.150	0.050	0.010
0	-1.2E-11	-1.2E-11	-6.2E-13	-1.6E-12	-1.5E-11	4.0E-12	-3.2E-12	-6.0E-13
1	-2.8E-11	-2.8E-11	-3.3E-11	1.4E-11	7.5E-11	-5.0E-10	2.0E-11	2.0E-11
2	-1.9E-10	-1.9E-10	-1.5E-11	-1.4E-10	-9.5E-11	-1.5E-10	-7.9E-11	-1.1E-11
3	2.2E-10	1.8E-10	-3.4E-11	-2.4E-10	-3.5E-10	-4.2E-10	9.6E-11	1.3E-11
4	5.9E-10	4.2E-10	-2.8E-11	-2.2E-09	-5.9E-10	-5.3E-10	-5.4E-10	-3.9E-10
5	-2.5E-10	-3.6E-10	1.6E-09	-9.9E-10	-3.4E-09	-9.3E-10	-1.9E-09	2.8E-10
6	9.5E-10	1.6E-09	3.7E-09	-8.3E-09	-1.0E-08	-2.8E-09	-5.4E-09	-1.8E-10
7	2.1E-08	1.8E-08	2.9E-08	-3.1E-08	-1.3E-08	-1.4E-08	-4.3E-09	5.2E-09
8	6.1E-08	6.4E-08	-4.8E-08	-1.0E-07	-4.1E-08	-3.1E-08	-8.4E-09	1.1E-08
9	1.4E-07	1.4E-07	2.4E-07	-3.8E-07	-1.5E-07	-6.4E-08	-3.5E-08	-1.8E-07
10	3.6E-07	3.5E-07	6.0E-07	-7.6E-07	-2.9E-07	-1.6E-07	-2.9E-08	-4.9E-07
11	7.6E-07	7.8E-07	1.6E-06	-1.0E-06	-3.1E-07	-4.9E-08	6.5E-08	-6.0E-07
12	1.4E-06	1.4E-06	2.7E-06	-2.0E-06	-1.0E-06	-2.5E-07	1.1E-07	-7.7E-07
13	2.7E-06	2.7E-06	4.3E-06	-3.6E-06	-1.9E-06	-3.7E-07	3.3E-07	-5.7E-07
14	4.2E-06	4.2E-06	5.9E-06	-5.0E-06	-1.6E-06	4.2E-07	1.0E-06	5.5E-07
15	6.7E-06	6.7E-06	9.0E-06	-2.9E-05	-2.2E-06	-9.3E-07	6.0E-07	3.1E-06
16	8.5E-06	8.6E-06	1.0E-05	-1.4E-05	-1.5E-06	2.2E-06	2.7E-06	8.4E-06
17	1.2E-05	1.2E-05	1.3E-05	-1.4E-05	-8.8E-06	1.4E-07	2.7E-06	1.3E-05
18	1.5E-05	1.5E-05	1.6E-05	3.1E-05	-1.3E-05	-8.9E-07	2.6E-06	6.6E-06
19	1.7E-05	1.7E-05	1.9E-05	3.8E-05	-1.7E-05	-1.4E-07	3.0E-06	-8.4E-06
20	2.0E-05	2.1E-05	2.1E-05	3.3E-05	-2.1E-05	1.6E-06	5.3E-06	-2.1E-05
21	2.4E-05	2.4E-05	2.2E-05	2.3E-05	-1.4E-05	9.4E-06	1.0E-05	-2.1E-05
22	2.5E-05	2.6E-05	2.3E-05	3.8E-05	2.0E-05	3.4E-05	6.8E-06	-8.6E-06
23	2.5E-05	2.6E-05	3.2E-05	5.2E-05	7.7E-05	4.3E-06	1.9E-06	-7.1E-05
24	2.9E-05	3.1E-05	2.7E-05	3.5E-05	7.4E-06	2.2E-05	1.6E-05	-6.5E-05
25	2.5E-05	2.9E-05	2.7E-05	6.0E-05	7.1E-05	1.0E-05	-4.0E-06	-1.2E-05
26	2.6E-05	3.2E-05	2.8E-05	3.8E-05	2.4E-05	3.5E-05	9.7E-06	4.0E-05
27	1.9E-05	2.7E-05	3.1E-05	5.2E-05	9.2E-05	3.7E-06	-1.8E-06	3.1E-05
28	1.5E-05	2.7E-05	2.5E-05	8.0E-05	6.2E-05	3.3E-05	-2.3E-05	6.3E-05
29	8.8E-06	2.5E-05	2.4E-05	9.7E-05	3.7E-05	5.1E-05	-2.1E-05	2.7E-05
30	-7.7E-06	1.7E-05	2.1E-05	4.6E-05	3.1E-05	1.5E-05	-1.6E-06	-2.4E-05
31	-2.3E-05	1.2E-05	1.6E-05	4.6E-05	3.8E-05	-2.2E-06	-2.5E-05	-6.5E-05
32	-4.3E-05	5.8E-06	3.3E-06	5.0E-05	7.7E-05	-5.4E-06	-4.9E-05	-9.5E-05
33	-7.2E-05	-3.4E-06	-2.4E-06	6.1E-05	6.5E-05	7.7E-07	-7.1E-05	-1.2E-04
34	-1.1E-04	-1.4E-05	-9.7E-06	7.2E-05	5.4E-05	9.3E-06	-9.0E-05	-1.4E-04

of radiative transfer Eq. (A48) should be omitted. Omitting the terms with convective variables Eq. (A45) becomes

$$\frac{d}{d\ln r}(P_g y_1 + \frac{1}{3}E_r y_5) - \frac{GM_r\rho}{r}(4 + \frac{r^3\omega^2}{GM_r})y_3 = 0. \quad (9)$$

At the same time, the equation of total energy conservation, Eq. (A46) and the equation of energy conservation for radiation field is replaced by the adiabatic and radiative equilibrium relation:

$$y_2 = \nabla^*_{ad} y_1, \quad (10)$$

$$y_5 = 4y_2. \quad (11)$$

Equations (A44), (9), (10) and (11) form a set of equations of adiabatic oscillations with 4 dependent variables (y_1, y_2, y_3 and y_5). The bottom and surface boundary conditions are Eqs. (A64) and (A69) separately. To minimize the numerical errors, we adopt the same differencing scheme and the same Henyey's iteration method in the calculations of both adiabatic and non-adiabatic oscillations. Since we are interested in the differences between the correspondent frequencies of adiabatic and non-adiabatic oscillations, the major part of the errors introduced by the differencing scheme and the solving method will cancel each other. Therefore, we think that the results are better.

3.2.3. The influence of the departure from radiative equilibrium on the p-mode oscillations

Unno and Spiegel (1966) have pointed out that, generally speaking, the radiative field and gas are not in equilibrium. They pro-

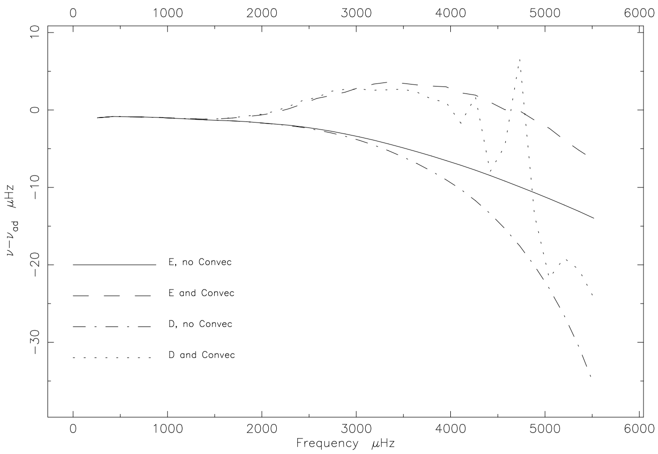

Fig. 4. The frequency differences between the non-adiabatic and adiabatic oscillations, $\nu - \nu_{ad}$ *vs* frequency. Other notations are the same as in Fig. 1.

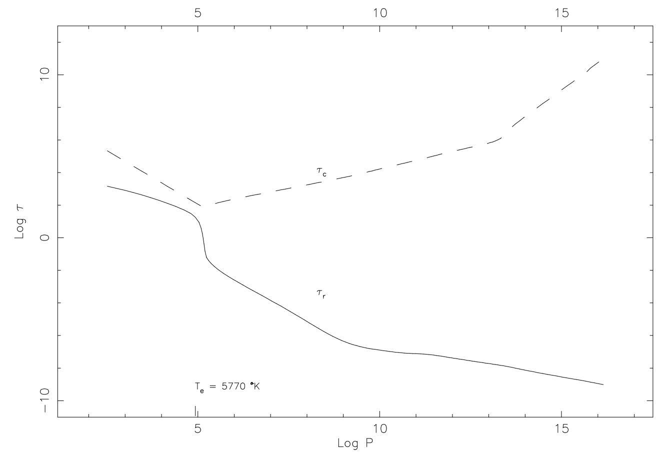

Fig. 5. The local convective inertia time-scale τ_c (Eq.38) and the radiative smoothing time of temperature perturbation, $\tau_r = C_{pT}/c\kappa E_r$ $vs\ logP$ for the solar envelope model.

posed a generalized Eddington approximation to treat the radiative relaxation problems of static temperature fluctuations. They argued that the resulting equations reduce to the exact equations for the problem of radiative relaxation small temperature fluctuations in the limits of both large and small optical thickness of perturbation, therefore it can be expected that they are reasonably accurate over the whole range of optical thickness. Mihalas (1984) generalized the Unno-Spiegel's formalism to the moving fluids. Ando and Osaki used the Unno-Spiegel's generalized Eddington approximation to calculate the solar 5-min oscillations. They found that many of solar p-modes are overstable and that the highest growth rates occur for nonradial p-modes having frequencies of about 5-min. After that, Christensen-Dalsgaard and Frandsen (1983) pointed out that Ando and Osaki had omitted the departures from radiative equilibrium in their calculation of the equilibrium models, and that, once the departure is considered, all the p-modes become pulsational stable.

In the present paper, the basic equations (Xiong, 1989) used for calculation of the solar non-adiabatic pulsation are a natural generalization of Mihalas' radiative hydrodynamic equations. Unno-Spiegel and Mihalas' theory are only available for pure radiative fluids. We generalized it to the include turbulent convection. Within the Eddington approximation, our theory has treated non-radiative equilibrium strictly by completely separating treatment of the radiation field and of the gas, and coupling the two by the absorption and radiation of gas, as shown by Eqs. (A7) and (A8).

To study the influence of non-radiative equilibrium on the stabilities of the solar p-mode oscillations, we have computed non-adiabatic oscillations with two different treatments of radiation:

(i). Strict consideration of the effects of non-radiative equilibrium

This uses the equations given in Sect 2. Gas and radiation field are described separately.

(ii). Omitting the effects of non-radiative equilibrium

That means assuming that gas and radiation are in thermal equilibrium states, $E_r \equiv aT^4$, namely, returning to the radiative diffusion approximation. At such circumstance, we only need to force the equilibrium quantities $E_r \equiv aT^4$, and the pulsational variable $y_5 = 4y_2$ in the calculation of pulsation. After doing so, the equations are reduced, from the original order 11, to order 10. If the coupling between convection and pulsation is neglected, the equations will reduce further to order 4, as usual. These results are listed in the 7th - 10th columns of Table 1.

Comparing the results of diffusion approximation, where the departure from radiative equilibrium has been neglected, with that of the Eddington approximation, where the departure from radiative equilibrium has been included, we can see that the effects of non-radiative equilibrium affect the solar p-mode oscillations significantly. However, they usually only alter the value of the stability coefficients but not their sign.

The influence of non-radiative equilibrium and non-adiabatic effects on the p-mode oscillations increases with the increase of frequency of the p-mode as shown in Fig. 1 and Fig. 4. This frequency dependence indicates that the influence of the solar atmosphere, where the non-adiabatic effects and the effects of non-radiative equilibrium are larger, on the oscillations of p-modes increases with their frequency.

In the solar atmosphere the convective flux is always neglected. From the conservation equation of the gas thermal energy (A76), we obtain the linear equation of oscillation (A77). The radiative smoothing time-scale τ_r versus lnP_g is plotted in Fig. 5. In the solar atmosphere, the period of the solar 5-min oscillations and τ_r have the same magnitude. For the low-frequency p-modes, whose $\omega\tau_r \ll 1$, from Eq. (A77) we have

$$y_5 = 4y_2. \quad (12)$$

namely, the Eddington approximation approaches to the diffusion approximation. Conversely, for the high frequency p-modes, where $\omega\tau_r \gg 1$, from Eq. (A77) we have

$$y_2 = \nabla_{ad} y_1, \tag{13}$$

the Eddington approximation approaches the adiabatic one. That is the reason why the differences between the Eddington approximation and the diffusion approximation increase with the increasing of the p-mode frequencies.

4. Conclusion and discussions

The linear non-adiabatic oscillations of solar envelope models were calculated using a non-local time-dependent theory of convection. The results can be summarized as follows,

1) Non-adiabatic effects have a non-negligible influence on the frequencies of the solar 5-min oscillations. The differences between non-adiabatic and adiabatic eigenfrequencies reach a maximum at $\nu \sim 3400\mu H_z$ and decrease towards both the high and low frequency to become finally negative. The maximum difference can reach several μH_z.

2) The departure from radiative equilibrium and the upper atmosphere of the Sun have significant influences on the stability and the frequencies of the solar 5-min oscillations. The influence increases with increasing frequency. The results for high-order p-mode with $\nu \gtrsim 4500\mu H_z$ are less reliable due to the uncertainty of the structure of upper atmosphere. The radiation-hydrodynamic equations (Mihalas 1984; Xiong 1989) based on the generalized Eddington approximation (Unno & Spiegel 1966) are more accurate than the radiative diffusion approximation for theoretical calculations of solar oscillations.

3) The influence of radiation pressure on the solar oscillations is negligible.

4) Turbulent pressure is a de-stabilization factor. The damping caused by turbulent viscosity increases more rapidly with increasing of frequency than the excitation by turbulent pressure does. Turbulent viscosity is the dominant factor of damping for the solar 5-min oscillations.

5) The effects of radiative energy transport on the stability of the solar 5-min oscillations are much smaller than the effects of convective flux. The thermodynamic coupling between convection and oscillations is the chief excitation mechanism of the solar 5-min oscillations. The excitation region lies predominantly in the super-adiabatic convection zone under the photosphere.

6) The solar 5-min oscillations may be excited by convection.

Convection is the key for understanding the properties and excitation of the solar 5-min oscillations. The statistical theory of non-local time-dependent convection is derived from the radiation-hydrodynamics and turbulence theory. Therefore we can expect it describe finely the dynamic behavior of convection. The only uncertain assumption used in the present non-local time-dependent convection theory is the gradient-type diffusion approximation of the triple correlations of the turbulent velocity and temperature fluctuations representing the non-local properties of convection. Recently, following Canuto (1993) we derived a set of dynamic equations for the triple correlations (Xiong et al, 1995). The new theory gives a theoretical ground for the gradient-type diffusion approximation. It shows that it is a good first order approximation.

Another uncertainty is due to the difficulty of numerical calculations. There are fast spatial oscillations in the convective variables and in the luminosity in our calculations. The origin of these spatial oscillations is very similar to that in the calculations of stellar pulsation with a local-convection theory. While the convection speed decreases rapidly in the overshooting zone, the inertia time-scale for convection increase rapidly. In the region where $\omega\tau_c \gg 1$ the non-local convective diffusion terms approach zero. Then the dynamical behaviour of convection is very similar to that described by local convection theory. We cannot yet estimate quantitatively the errors brought by the spatial oscillations. But from the fact that the linear pulsational stability coefficients given by the calculation of pulsation are very close to those obtained by the calculation of accumulate works, the effects are far smaller than could be imagined a priori. The influences of these spatial oscillations and how to get rid of them is still a problem to be investigated.

Appendix A: equations of radial nonadiabatic oscillations of stars

To avoid unnecessary repetition, we do not list the basic radiative- hydrodynamic equations for stellar oscillations here (Xiong, 1989, 1994). We only point out here that:

1). The departure from radiative equilibrium has been considered; radiation and gas have been described separately.

2). The non-isotropic component of the turbulent Reynolds stress has been included.

3). The dynamic equation for $\overline{u'^i w'^k T'/\overline{T}}$ is now in a symmetric form for subscripts (superscripts) i and k.

These modifications does not alter the results in our earlier papers, at least for the problems of steady convection. The detailed derivation can be found in our earlier paper (Xiong, 1989, 1994; Xiong et al. 1995).

A.1. Equations of radial oscillations of stars

Our basic equations are appropriate for both radial and nonradial oscillations of stars. For radial oscillations of stars, the Poisson equation become:

$$\frac{\partial\Phi}{\partial r} = \frac{GM_r}{r^2}, \tag{A1}$$

and the vectors u^k, V^k, F_r^k, $\overline{u'^k w_i' w'^i}$ and $\overline{u'^k (T'/\overline{T})^2}$ have only radial components u, V, F_r, $\overline{u'^1 w_i' w'^i}$ and $\overline{u'^1 (T'/\overline{T})^2}$.

We choose mass M_r, which is a Lagrangian invariant during pulsation, as the independent spatial variable, and introduce the following dependent convective variables,

$$L_1 = 2\pi r^2 \rho \overline{u'^1 w_i' w'^i}/3, \tag{A2}$$

$$L_3 = 4\pi r^2\rho^2 C_p^2(1+e_4)^2\overline{w'^1(\frac{T'}{\overline{T}})^2}, \tag{A3}$$

$$L_5 = 4\pi r^2\rho C_p(1+e_4)\overline{w'^1 w'_1\frac{T'}{\overline{T}}}. \tag{A4}$$

The equations of stellar radial oscillations can be written as follows:

$$\frac{\partial r}{\partial M_r} = \frac{1}{4\pi r^2\rho}, \tag{A5}$$

$$\frac{Du}{Dt} + 4\pi r^2\frac{\partial}{\partial M_r}(P_g + \rho x^2 + \frac{E_r}{3}) + \frac{4\pi}{r}\frac{\partial}{\partial M_r}(\rho r^3 \mathscr{X}^{\cdot 11})$$

$$+\frac{GM_r}{r^2} = 0, \tag{A6}$$

$$C_p\frac{DT}{Dt} + \frac{1}{\rho}\frac{DE_r}{Dt} + \frac{3}{2}\frac{Dx^2}{Dt} - \frac{B}{\rho}\frac{DP_g}{Dt} - \frac{1}{\rho}(x^2 + \frac{4}{3}\frac{E_r}{\rho})\frac{D\rho}{Dt} + \frac{GM_r BV\tau_c}{4r^2}\frac{\partial}{\partial \ln r}(\frac{u}{r}) + \frac{\partial}{\partial M_r}(L_r + L_c + 3L_1) = 0, \tag{A7}$$

$$\frac{DE_r}{Dt} - \frac{4}{3}\frac{E_r}{\rho}\frac{D\rho}{Dt} + \rho\frac{\partial}{\partial M_r}(L_r + L_{c,r}) + \frac{B\rho\chi L_r V}{4\pi c r^2}$$

$$+c\rho\kappa(E_r - aT^4) = 0, \tag{A8}$$

$$L_r = -\frac{16\pi^2 c r^4}{3\chi}\frac{\partial E_r}{\partial M_r}, \tag{A9}$$

$$\tau_c[\frac{DL_1}{Dt} - L_1\frac{D}{Dt}\ln(\rho r^2)] + L_1$$

$$= -\frac{4\sqrt{3}\pi^2 c_2\rho P_g r^6 x^2}{GM_r}\frac{\partial x}{\partial M_r}, \tag{A10}$$

$$\tau_c\{\frac{DL3}{Dt} - 2L_3\frac{D}{Dt}\ln[\rho C_p r^2(1+e_4)]\} + L_3$$

$$= -\frac{4\sqrt{3}\pi^2 c_2\rho^2 C_p^2(1+e_4)^2 P_g r^6 x}{GM_r}\frac{\partial Z}{\partial M_r}, \tag{A11}$$

$$\tau_c\{\frac{DL5}{Dt} - L_5\frac{D}{Dt}\ln[\rho C_p r^2(1+e_4)]\} + L_5$$

$$= -\frac{4\sqrt{3}\pi^2 c_2\rho C_p(1+e_4)P_g r^6 x}{GM_r}\frac{\partial V}{\partial M_r}, \tag{A12}$$

$$\frac{3}{2}\frac{Dx^2}{Dt} - \frac{x^2}{\rho}\frac{D\rho}{Dt} - BV\{\frac{GM_r}{r^2}[1 - \frac{\tau_c}{4}\frac{\partial}{\partial \ln r}(\frac{u}{r})] + \frac{Du}{Dt}\}$$

$$+3\frac{\partial L_1}{\partial M_r} + 1.56\frac{GM\rho x^3}{c_1 r^2 P_g} = 0, \tag{A13}$$

$$(1+e_4)\frac{DZ}{Dt} + 2Z(f_2\frac{D\ln T}{Dt} - f_1\frac{D\ln P_g}{Dt} + 4e_3\frac{D\ln E_r}{Dt}) + 8\pi r^2\rho V[(1+e_2)\frac{\partial \ln T}{\partial M_r} - (\nabla_{ad} + e_1)\frac{\partial}{\partial M_r}\ln P_g + e_3\frac{\partial}{\partial M_r}\ln E_r] + \frac{1}{\rho C_p^2(1+e_4)}\frac{\partial L_3}{\partial M_r} + 2\frac{GM\rho(x+x_c)Z}{c_1 r^2 P_g} = 0, \tag{A14}$$

$$(1+e_4)[\frac{DV}{Dt} - BZ(\frac{GM_r}{r^2} + \frac{Du}{Dt})] + V[4\pi r^2\rho(1+e_4)\frac{\partial u}{\partial M_r} + f_2\frac{D\ln T}{Dt} - f_1\frac{D\ln P_g}{Dt} + 4e_3\frac{D\ln E_r}{Dt}] + 4\pi r^2\rho x^2[(1+e_2)\frac{\partial \ln T}{\partial M_r} - (\nabla_{ad} + e_1)\frac{\partial}{\partial M_r}\ln P_g + e_3\frac{\partial}{\partial M_r}\ln E_r] + \frac{1}{C_p}\frac{\partial L_5}{\partial M_r} + \frac{GM\rho(2.56x + x_c)V}{c_1 r^2 P_g} = 0. \tag{A15}$$

Here x^2, Z and V are the auto- and cross-correlations of turbulent velocity and temperature fluctuations:

$$x^2 = \frac{1}{3}\overline{w'_i w'^i}, \tag{A16}$$

$$Z = \overline{(T'/\overline{T})^2}, \tag{A17}$$

$$V^i = \overline{w'^i T'/\overline{T}}, \tag{A18}$$

where

$$w'^i = \rho u'^i/\overline{\rho}. \tag{A19}$$

u^i (u_i) is the i-th contravariant (covariant) component of velocity vector. A pair of the same superscript and subscript i (j, k) here implies the sum for i (j, k) from 1 to 3. A variable with a prime means its turbulent fluctuation, while an overbar or overline indicates an average value. All other variables and the state parameters are their own average value after an average procedure over the turbulent fluctuations, and the overbar has been omitted for simplicity here and below.

And

$$L_r = 4\pi r^2 F_r, \tag{A20}$$

$$L_c = L_{c,g} + L_{c,r}, \tag{A21}$$

$$L_{c,g} = 4\pi r^2 F_{c,g} = 4\pi r^2\rho C_p T V, \tag{A22}$$

$$L_{c,r} = 4\pi r^2 F_{c,r} = 16\pi(4+B)r^2 E_r V/3. \tag{A23}$$

$\mathscr{X}^{ij}$ is the nonisotropic component of the turbulent Reynolds stress due to the buoyancy and the shear motion of fluid:

$$\overline{w'^i w'^j} = g^{ij}x^2 + \mathscr{X}^{ij}. \tag{A24}$$

From the dynamic equation for $\overline{w'^i w'^j}$, it is not difficult to get the dynamic equation of $\mathscr{X}^{ij}$ (Xiong et al., 1995),

$$\frac{D\mathscr{X}^{ij}}{Dt} + x^2(g^{i\alpha}\nabla_\alpha u^j + g^{j\alpha}\nabla_\alpha u^i - \frac{2}{3}g^{ij}\nabla_\alpha u^\alpha) + \mathscr{X}^{i\alpha}\nabla_\alpha u^j + \mathscr{X}^{j\alpha}\nabla_\alpha u^i - \frac{2}{3}g^{ij}\mathscr{X}^{\alpha\beta}\nabla_\alpha u_\beta - \alpha(g^{i\alpha}V^j + g^{j\alpha}V^i - \frac{2}{3}g^{ij}V^\alpha)(\nabla_\alpha\Phi + \frac{Du_\alpha}{Dt}) = -\frac{16}{3}\gamma_1 x\mathscr{X}^{ij}, \tag{A25}$$

where the terms with gradient of velocity represent the turbulent viscosity. We can see that they are very similar to the Stokes formula of viscous fluids. For radial oscillations, $\mathscr{X}^{ij}$ has only one independent component,

$$\mathscr{X}^{\cdot 11} = -2\mathscr{X}^{\cdot 22} = -2\mathscr{X}^{\cdot 33}. \tag{A26}$$

From Eq. (A25), we have

$$\frac{D\mathscr{X}^{11}}{Dt}+\frac{16}{3}\gamma_1 x\mathscr{X}^{11}$$
$$=\frac{4}{3}\{BV[\frac{Du}{Dt}+\frac{GM_r}{r^2}(1-\frac{\tau_c}{4}(\frac{\partial u}{\partial r}+\frac{u}{2r}))]-x^2\frac{\partial}{\partial\ln r}(\frac{u}{r})\}. \quad (A27)$$

Some symbols used here are defined as follows:

$$\frac{D}{Dt}=\frac{\partial}{\partial t}+u^k\nabla_k, \quad (A28)$$

$$e_1=\frac{4AE_r}{3\rho C_p T}, \quad (A29)$$

$$e_2=\frac{4BE_r}{3\rho C_p T}, \quad (A30)$$

$$e_3=\frac{E_r}{\rho C_p T}, \quad (A31)$$

$$e_4=\frac{4E_r(3+B)}{3\rho C_p T}, \quad (A32)$$

$$f_1=B_T\nabla_{ad}+\frac{4E_r}{3\rho C_p T}(4A-BB_T), \quad (A33)$$

$$f_2=1+B[\frac{4E_r}{3\rho C_p T}(4+B_T)-1]+C_{p,T}, \quad (A34)$$

$$\gamma_1=\eta_e k_e=\sqrt{3}\eta_e k_{e1}=\sqrt{3}\eta_e/l_{e1}=0.78\rho GM_r/c_1 r^2 P_g, \quad (A35)$$

$$\gamma_3=(1+x_c/x)k_e, \quad (A36)$$

$$\gamma_5=\gamma_1+\gamma_3/2, \quad (A37)$$

$$\tau_c=1/\gamma_1 x=c_1 H_P/\sqrt{3}\eta_e x=c_1 r^2 P_g/\sqrt{3}\eta_e\rho GM_r x, \quad (A38)$$

$$x_c=3acGM_rT^3/c_1\chi\rho C_p r^2 P_g, \quad (A39)$$

where τ_c is the time-scale of turbulent convection (Xiong, 1977). x_c/x is the effective Peclet number measuring the efficiency of convective energy transport. η_e is the Heisenberg turbulent eddy coupling constant. $\eta_e=0.45$ in the present and earlier papers. The choice of η_e has no significant influence on our results, because there are two adjustable convective parameters c_1 and c_2 in our nonlocal statistical theory of convection. k_{e1} and l_{e1} are the average radial wave number and size of energy-containing eddies respectively. It is assumed that l_{e1} is directly proportional to the local pressure scale height H_P,

$$l_{e1}=c_1 H_P\approx c_1 r^2 P_g/\rho GM_r, \quad (A40)$$

where c_1 is the convective parameter in relation to the turbulent dissipation due to the molecular viscosity.

Other symbols have their usual meanings. ρ, P_g, T are the gas density, pressure and temperature respectively, Φ is the gravitational potential, ε, C_p, κ and χ are the energy generation rate, the specific heat at constant pressure, the thermal absorption and the total extinction per gram (the sum of the scattering and the thermal absorption), c is the velocity of light, a is the radiation coefficient. E_r and F_r^i are the radiation energy density and the radiation flux vector in the comoving frame, A, B and ∇_{ad} are the compressibility, expansivity coefficient and adiabatic temperature gradient respectively:

$$A=(\frac{\partial\ln\rho}{\partial\ln P_g})_T, \qquad B=-(\frac{\partial\ln\rho}{\partial\ln T})_{P_g},$$

$$\nabla_{ad}=(\frac{\partial\ln T}{\partial\ln P_g})_{ad}=\frac{BP_g}{\rho C_p T}. \quad (A41)$$

The subscript g (r) denotes that the value belongs to the gas (radiation field)(except for M_r). The subscript T and P appended on the state parameters represent their logarithmic partial derivative for T and P_g respectively, for example,

$$B_T=(\tfrac{\partial\ln B}{\partial\ln T})_{P_g}, \qquad B_P=(\tfrac{\partial\ln B}{\partial\ln P_g})_T,$$
$$C_{p,T}=(\tfrac{\partial\ln C_p}{\partial\ln T})_{P_g}, \qquad C_{p,P}=(\tfrac{\partial\ln C_p}{\partial\ln P_g})_T. \quad (A42)$$

A.2. Linearized equations of the nonadiabatic oscillations of stars

Putting all the Lagrangian variables in the form of the sum of the equilibrium and the pulsational components,

$$Y_j(M_r t)=Y_{j,0}(M_r)+\delta Y_j(M_r)e^{i\omega t}, \quad j=1-11, \quad (A43)$$

and substituting Eq. (A42) into Eqs. (A5)–(A15), after separation of the equilibrium and pulsational components, we can obtain the equations for the equilibrium model (omitted here, please refer to Xiong & Cheng, 1992), and the following linearized equations of radial nonadiabatic oscillations of stars,

$$\frac{dy_3}{d\ln r}+Ay_1-By_2+3y_3=0, \quad (A44)$$

$$\begin{aligned}&\tfrac{d}{d\ln r}[(P_g+A\rho x^2)y_1+\rho x^2(2y_6-By_2)+\tfrac{E_r}{3}y_5]+\\ &\quad\tfrac{4}{3}\tfrac{1}{r^3}\tfrac{d}{d\ln r}\{[GM_r\rho rBV\tau_c^*+\tfrac{i\omega\tau_c^*}{1+i\omega\tau_c^*}(\rho r^3x^2\\ &\quad+GM_r\rho rBV\tau_c)](Ay_1-By_2+3y_3)\\ &\quad+\tfrac{\tau_c^*}{1+i\omega\tau_c^*}GM_r\rho rBV[y_{10}-(2+\tfrac{r^3\omega^2}{GM_r}\\ &\quad+2i\omega\tau_c^*)y_3]\}-[4\tfrac{1}{r^3}\tfrac{d}{d\ln r}(GM_r\rho rBV\tau_c^*)\\ &\quad+4\tfrac{GM_r\rho}{r}+\rho r^2\omega^2]y_3=0,\end{aligned} \quad (A45)$$

$$\begin{aligned}&\tfrac{d}{d\ln r}\{\tfrac{L_{c,g}}{L_0}[(A+C_{p,P})y_1+(1-B+C_{p,T})y_2]+\tfrac{L_r}{L_0}y_4+\\ &\quad\tfrac{L_{c,r}}{L_0}[\tfrac{B}{4+B}(B_Py_1+B_ty_2)+y_5]\\ &\quad\tfrac{L_c}{L_0}(2y_3+y_{10})+3\tfrac{L_1}{L_0}y_7\}-i\omega\tfrac{4\pi r^3\rho C_pT}{L_0}\\ &\quad[(\nabla_{ad}+A\tfrac{\rho x^2+4E_r/3}{\rho C_pT}+\tfrac{GM_rBV\tau_c}{4r^2})y_1-\\ &\quad(1+B\tfrac{\rho x^2+4E_r/3}{\rho C_pT}+\tfrac{GM_rBV\tau_c}{4r^2})y_2+\tfrac{3}{4}\tfrac{GM_rBV\tau_c}{4r^2C_pT}y_3\\ &\quad-\tfrac{E_r}{\rho C_pT}y_5-\tfrac{3x^2}{C_pT}y_6]=0,\end{aligned} \quad (A46)$$

$$\begin{aligned}&\frac{d}{d\ln r}\{\frac{L_{c,r}}{L_0}[\frac{B}{4+B}(B_P y_1 + B_T y_2) + 2y_3 + y_5 + y_{10}]\\&\quad + \frac{L_r}{L_0}y_4\}\\&\quad - \frac{4\pi r^3 c\rho\kappa E_r}{L_0}\{[i\omega\frac{4A}{3c\rho\kappa} + (\frac{aT^4}{E_r} - 1)\kappa_P\\&\quad - \frac{BVL_r}{4\pi r^2 c^2 E_r}\\&\quad (B_P + \kappa_P)]y_1\\&\quad + [\frac{4aT^4}{E_r} + (\frac{aT^4}{E_r} - 1)\kappa_T - \frac{BVL_r}{4\pi r^2 c^2 E_r}(B_T + \kappa_T)\\&\quad - i\omega\frac{4B}{3c\rho\kappa}]y_2\\&\quad + \frac{BVL_r}{4\pi r^2 c^2 E_r}(2y_3 - y_4 - y_{10}) - (1 + \frac{i\omega}{c\rho\kappa})y_5\} = 0,\end{aligned} \qquad (A47)$$

$$\frac{dy_5}{d\ln r} - \frac{dE_r}{d\ln r}(\chi_P y_1 + \chi_T y_2 - 4y_3 + y_4 - y_5) = 0, \qquad (A48)$$

$$\begin{aligned}&\frac{\sqrt{3}\pi c_2 P_g r^3 x^3}{GM_r}\frac{dy_6}{d\ln r} - L_1\{[1 + A(1 + i\omega\tau_c)]\\&\quad y_1 - B(1 + i\omega\tau_c)]y_2\\&\quad + (6 + 2i\omega\tau_c)y_3 + 3y_6 - (1 + i\omega\tau_c)y_7\} = 0,\end{aligned} \qquad (A49)$$

$$\begin{aligned}&\frac{\sqrt{3}\pi c_2\rho C_p^2(1+e_4)^2 P_g r^3 xZ}{GM_r}\frac{dy_8}{d\ln r} - L_3\{[1 + 2(1 + i\omega\tau_c)h_1]y_1\\&\quad + 2(1 + i\omega\tau_c)h_2 y_2 + (6 + 2i\omega\tau_c)y_3\\&\quad + 2(1 + i\omega\tau_c)h_3 y_5 + y_6 + y_8\\&\quad - (1 + i\omega\tau_c)y_9\} = 0,\end{aligned} \qquad (A50)$$

$$\begin{aligned}&\frac{\sqrt{3}\pi c_2 C_p(1+e_4)P_g r^3 xV}{GM_r}\frac{dy_{10}}{d\ln r} - L_5\{[1 + (1 + i\omega\tau_c)h_1]y_1\\&\quad + (1 + i\omega\tau_c)h_2 y_2 + (6 + 2i\omega\tau_c)y_3\\&\quad + (1 + i\omega\tau_c)h_3 y_5\\&\quad + y_6 + y_{10}\\&\quad - (1 + i\omega\tau_c)y_{11}\} = 0,\end{aligned} \qquad (A51)$$

$$\begin{aligned}&\frac{L_1}{L_0}\frac{dy_7}{d\ln r} + y_7\frac{d}{d\ln r}(\frac{L_1}{L_0}) + \frac{4\pi GM_r\rho r}{3L_0}\\&\quad \{[1.56(A - 1 - \tfrac{1}{2}i\omega\tau_c A)\frac{\rho x^3}{c_1 P_g}\\&\quad - BV(B_P + \frac{i\omega\tau_c A}{4})]y_1\\&\quad - B[1.56(1 - \tfrac{1}{2}i\omega\tau_c)\frac{\rho x^3}{c_1 P_g} + (B_T - \frac{i\omega\tau_c}{4})V]y_2\\&\quad + [BV(2 + \frac{r^3\omega^2}{GM_r} - \frac{3i\omega\tau_c}{4}) - 3.12\frac{\rho x^3}{c_1 P_g}]y_3\\&\quad + 4.56(1 + \tfrac{1}{2}i\omega\tau_c)\frac{\rho x^3}{c_1 P_g}y_6 - BVy_{10}\} = 0,\end{aligned} \qquad (A52)$$

$$\begin{aligned}&\frac{1}{4\pi r^2\rho^2 C_p^2(1+e_4)}(L_3\frac{dy_9}{d\ln r} + y_9\frac{dL_3}{d\ln r}) - 2V[(\nabla_{ad} + e_1)\frac{dy_1}{d\ln r}\\&\quad - (1 + e_2)\frac{dy_2}{d\ln r} - e_3\frac{dy_5}{d\ln r}]\\&\quad - 2\{D_1 V + \frac{A + C_{p,P} + h_1}{8\pi r^2\rho^2 C_p^2(1+e_4)}\frac{dL_3}{d\ln r} + \frac{\rho GM_r}{c_1 r P_g}\\&\quad Z[x + x_c + 0.78i\omega\tau_c f_1 x]\}y_1\\&\quad - 2\{D_2 V + \frac{C_{p,T} - B + h_2}{8\pi r^2\rho^2 C_p^2(1+e_4)}\frac{dL_3}{d\ln r}\\&\quad - 0.78i\omega\tau_c f_2\frac{\rho GM_r}{c_1 r P_g}xZ]\}y_2\\&\quad - 4[DV + \frac{\rho GM_r}{c_1 r P_g}(x + x_c)Z]y_3\\&\quad - 2[D_3 V + \frac{h_3}{8\pi r^2\rho^2 C_p^2(1+e_4)}\frac{dL_3}{d\ln r}\\&\quad - 3.12i\omega\tau_c e_3\frac{\rho GM_r}{c_1 r P_g}xZ]y_5\\&\quad + \frac{\rho GM_r}{c_1 r P_g}Z\{2xy_6 + [2(x + x_c)\\&\quad + 0.78i\omega\tau_c(1 + e_4)x]y_8\}\\&\quad - 2DVy_{10} = 0,\end{aligned} \qquad (A53)$$

$$\begin{aligned}&\frac{1}{4\pi r^2\rho C_p}(L_5\frac{dy_{11}}{d\ln r} + y_{11}\frac{dL_5}{d\ln r}) - x^2[(\nabla_{ad} + e_1)\frac{dy_1}{d\ln r}\\&\quad - (1 + e_2)\frac{dy_2}{d\ln r} - e_3\frac{dy_5}{d\ln r}]\\&\quad + 0.78i\omega\tau_c(1 + e_4)\frac{\rho GM_r}{c_1 r P_g}xV\frac{dy_3}{d\ln r}\\&\quad - \{D_1 x^2 + \frac{A + C_{p.P}}{4\pi r^2\rho C_p}\frac{dL_5}{d\ln r} + \frac{\rho GM_r}{c_1 r P_g}V[2.56x + x_c\\&\quad + 0.78i\omega\tau_c f_1 x] - (1 + e_4)\\&\quad \frac{BZGM_r}{r}(2A + C_{p.P} - B_p - h_1)\}y_1\\&\quad - \{D_2 x^2 + \frac{C_{p.T} - B}{4\pi r^2\rho C_p}\frac{dL_5}{d\ln r} + (1 + e_4)\\&\quad \frac{BZGM_r}{r}(2B - C_{p.T} + B_T + h_2)\\&\quad - 0.78i\omega\tau_c f_2 xV\frac{\rho GM_r}{c_1 r P_g}\}y_2\\&\quad - \{2Dx^2 + \frac{\rho GM_r V}{c_1 r P_g}[5.12x + 2x_c\\&\quad - 0.78i\omega\tau_c(1 + e_4)x]\\&\quad - (1 + e_4)\frac{BZGM_r}{r}(2 + \frac{r^3\omega^2}{GM_r})\}y_3\\&\quad - [D_3 x^2 + \frac{GM_r}{r}(e_4 BZ - 3.12i\omega\tau_c e_3\frac{\rho xV}{c_1 P_g})]y_5\\&\quad - (2Dx^2 - 2.56\frac{\rho GM_r xV}{c_1 r P_g})y_6 - \frac{GM_r}{r}BZ(1 + e_4)y_8\\&\quad + \frac{\rho GM_r V}{c_1 r P_g}[2.56x + x_c + 0.78i\omega\tau_c(1 + e_4)x]y_{10} = 0.\end{aligned} \qquad (A54)$$

Where y_j (j = 1—11) are the relative complex amplitudes,

$$\begin{aligned}&y_1 = \delta P_g/P_g, && y_2 = \delta T/T, && y_3 = \delta r/r,\\&y_4 = \delta L_r/L_r, && y_5 = \delta E_r/E_r, && y_6 = \delta x/x,\\&y_7 = \delta L_1/L_1, && y_8 = \delta Z/Z, && y_9 = \delta L_3/L_3,\\&y_{10} = \delta V/V, && y_{11} = \delta L_5/L_5,\end{aligned} \qquad (A55)$$

and,

$$\tau_c^* = 3\tau_c/16, \qquad (A56)$$

$$h_1 = (A + C_{p,P})/(1 + e_4) + h_3 BB_P/(3 + B), \qquad (A57)$$

$$h_2 = (C_{p,T} - B)/(1 + e_4) + h_3[BB_T/(3 + B) - 1], \qquad (A58)$$

$$h_3 = e_4/(1 + e_4), \qquad (A59)$$

$$D = (\nabla_{ad} + e_1)\frac{d\ln P_g}{d\ln r} - (1 + e_2)\frac{d\ln T}{d\ln r} - e_3\frac{d\ln E_r}{d\ln r}, \qquad (A60)$$

$$\begin{aligned}D_1 = &[(\nabla_{ad}\nabla_{ad,P} - (A + C_{p,P} - A_P)e_1]\frac{d\ln P_g}{d\ln r}\\&+ (A + C_{p,P} - B_P)e_2\frac{d\ln T}{d\ln r} + (A + C_{p,P})\\&e_3\frac{d\ln E_r}{d\ln r},\end{aligned} \qquad (A61)$$

$$\begin{aligned}D_2 = &[\nabla_{ad}\nabla_{ad,T} - (1 - B + C_{p,T} - A_T)e_1]\frac{d\ln P_g}{d\ln r}\\&+ (1 - B + C_{p,T} - B_T)e_2\frac{d\ln T}{d\ln r}\\&+ (1 - B + C_{p,T})e_3\frac{d\ln E_r}{d\ln r},\end{aligned} \qquad (A62)$$

$$D_3 = e_3[\frac{4}{3}(A\frac{d\ln P_g}{d\ln r} - B\frac{d\ln T}{d\ln r}) - \frac{d\ln E_r}{d\ln r}], \qquad (A63)$$

and $\omega = \omega_r + i\omega_i$ is the complex angular frequency. Eqs. (A44) – (A54) form a complete set of linearized equations of radial nonadiabatic oscillations. Here one should notice that the Eq. (A45) have been modified to take account approximately of the nonisotropic Reynorlds stress and viscous stress of turbulent convection (Xiong et al., 1995). For defining the solution of the linearized pulsational equations we have to supply eleven boundary conditions and a normalization condition. If both of the surface and bottom boundaries are located at a layer sinking deeply into the convective overshooting zone, where $\omega\tau_c \gg 1$, the boundary conditions can be written as follows:

At bottom,

$$y_3 = 0, \tag{A64}$$

$$y_2 - \nabla^*_{ad} y_1 = 0, \tag{A65}$$

$$Ay_1 - By_2 + 2y_3 - y_7 = 0, \tag{A66}$$

$$2(h_1 y_1 + h_2 y_2 + y_3 + h_3 y_5) - y_9 = 0, \tag{A67}$$

$$h_1 y_1 + h_2 y_2 + 2y_3 + h_3 y_5 - y_{11} = 0, \tag{A68}$$

and at surface,

$$y_1 + (4 + \frac{R^3\omega^2}{GM_r}) y_3 = 0, \tag{A69}$$

$$[\chi_P(\frac{aT^4}{E_r} - 1) - i\omega\tau_r\nabla_{ad}]y_1 + [4\frac{aT^4}{E_r} + \chi_T(\frac{aT^4}{E_r} - 1) + i\omega\tau_r]y_2 - y_5 = 0, \tag{A70}$$

$$2y_3 - y_4 + y_5 = 0, \tag{A71}$$

$$y_3 = 1, \tag{A72}$$

$$Ay_1 - By_2 + 2y_3 - y_7 = 0, \tag{A73}$$

$$2(h_1 y_1 + h_2 y_2 + y_3 + h_3 y_5) - y_9 = 0, \tag{A74}$$

$$h_1 y_1 + h_2 y_2 + 2y_3 + h_3 y_5 - y_{11} = 0, \tag{A75}$$

where $\tau_r = C_pT/c\kappa E_r$ denotes the radiative smoothing-time of temperature perturbation and ∇^*_{ad} is the effective adiabatic temperature gradient,

$$\nabla^*_{ad} = (\nabla_{ad} + e_2)/(1 + e_4). \tag{A76}$$

Eqs. (A64), (A65) and (A69) - (A71) are the mechanical and thermal boundary conditions at the bottom and at the surface respectively, and Eqs. (A66) - (A68) and (A73) - (A75) are the convective boundary conditions. Eq. (A72) is the normalization condition.

We do not try to deduce in detail the above boundary conditions. Let us, however, give a brief demonstration. We have already assumed that both of the surface and bottom boundaries are located at a layer sinking deeply into the convective overshooting zone where $|\omega\tau_c| \gg 1$. Let $\omega\tau_c \to \infty$, the convective boundary conditions (A66) - (A68) and (A73) - (A75) can be obtained from Eqs. (A49) - (A51). Towards the surface and bottom boundaries , $\rho x^2/P_g$, $|L_1/L|$ and $|L_c/L|$ are much smaller than 1, therefore the terms with convective variables in Eqs. (A45) - (A47) can be neglected, namely the effects of convection on the mechanical and thermal boundary conditions are negligible. From the conservation equation of the gas thermal energy (Xiong, 1989),

$$C_p\frac{DT}{Dt} - \frac{B}{\rho}\frac{DP_g}{Dt} + c\kappa(aT^4 - E_r)$$

$$= \varepsilon - \frac{1}{\rho}\nabla_k(\rho C_p T V^k) + \frac{BV^k}{\rho}\nabla_k P_g + 2\gamma_1 x^3, \tag{A77}$$

where ε is the nuclear energy generation rate per gram, which is negligible in the solar envelope. Neglecting the terms on the right hand side of the equation, which are related to the nuclear energy generation and convection, and after linearization, we can obtain the boundary condition Eq. (A70).

$$[(\frac{aT^4}{E_r} - 1)\chi_P - i\omega\tau_r\nabla_{ad}]y_1 + [4\frac{aT^4}{E_r} + (\frac{aT^4}{E_r} - 1)\chi_T + i\omega\tau_r]y_2 - y_5 = 0. \tag{A78}$$

Note that $\omega\tau_r$ and $\left|aT^4/E_r - 1\right|$ are far smaller than 1 in the stellar interior, so we have

$$y_5 \approx 4y_2. \tag{A79}$$

Noting that $\left|4\pi r^3\rho C_p T\omega/L\right| \gg 1$ in the stellar interior and substituting Eq. (A79) into Eq. (A46), we have

$$y_2 \approx \nabla^*_{ad} y_1. \tag{A80}$$

Eq. (A79) or Eq. (A80) can be used as the bottom thermal boundary condition. For giants, the pulsational amplitude decreases rapidly towards the centre of star, therefore bottom boundary condition (A64) is a good approximation. The central region of the Sun has unnegligible influence on the frequencies of the low degree p-modes, so the frequencies listed in Table 1 are not very accurate. In order to get accurate frequencies, calculations for the complete solar model should be performed. However, the goal of the present paper is to investigate the pulsational stability and the influence of the nonadiabatic effects on the frequencies. For this we need only to calculate oscillations of the envelope models, because the nonadiabatic effects and the pulsational amplitude are very small in the central region, therefore, its influence can be neglected.

The surface boundary conditions have been already investigated in detail by Unno (1965), therefore the demonstration of the surface mechanical and thermal boundary conditions (A69) and (A71) is omitted here.

References

Ando, H. & Osaki, Y., 1975, PASJ, 27, 581

Antia, H., M., Chitre, S. M. & Narasimha, D., 1982, Solar Phys., 77, 303

Antia, H., M., Chitre, S. M. & Gough, D. O., 1987, in Advances in Helio- and Asteroseismology, IAU Symp. No. 123, p.371 Solar Phys., 77, 303

Baker, N. H. & Gough, D. O., 1979, ApJ, 234, 232

Balmforth, N. J., 1992a, MNRAS, 255, 603

Balmforth, N. J., 1992b, MNRAS, 255, 632

Balmforth, N. J. & Gough, D. O., 1989, in Seismology of the Sun and Sun-like Stars, Eds. Domingo, V. & Rolfe, E., ESA-286, p.47

Brown, T. M., Stebbins, R. T. & Hill, H. A., 1978, ApJ, 223, 324

Canuto, V. M., 1993, ApJ, 416, 331

Christensen-Dalsgaard, J. & Frandsen, S., 1983, Solar Phys. 82, 165

Däppen, W., Mihalas, D., Hummer, D. G. & Mihalas, B. W., 1988, ApJ, 332, 261
Gingerich, O., Noyes, R. W., Kalkofen, W. & Cuny, Y., 1971, Solar Phys., 18, 347
Goldreich, P. & Keeley, D. A., 1977, ApJ, 212, 243
Gough, D. O., 1976, in Problems of Stellar Convection, IAU Collq. No. 38, Eds. Spiegel, E. & Zahn, J-P., Springel-Verlag, Berlin, p.15
Gough, D. O., 1977, ApJ, 214, 196
Gough, D. O., 1980, in Nonradial and Nonlinear Stellar Pulsation, eds H. A. Hill & W. Dziembowski, p.273
Hill, H., 1985, ApJ, 290, 765
Hill, H., Tash, J. & Padin, C., 1986, ApJ, 304, 560
Hummer, D. G. & Mihalas, D., 1988, ApJ, 331, 794
Libbrecht, K. G., 1988, ApJ, 334, 510
Mihalas, W. M., 1984, ApJ, 284, 299
Mihalas, D., Däppen, W. & Hummer, D. G., 1988, ApJ, 331, 815
Spiegel, E. A., 1963, ApJ, 138, 216
Travis, L. D. & Matsushima, S., 1973, ApJ, 180, 975
Unno, W., 1965, PASJ 17, 205
Unno, W., Spiegel, E. A., 1966, PASJ 18, 85
Xiong, D. R., 1977, Acta Astron. Sinica 18, 86 (Engl. trans. in Chinese Astron. 2, 118)
Xiong, D. R., 1979, Acta Astron. Sinica 20, 238 (Engl. trans. in Chinese Astron. 4, 238)
Xiong, D. R., 1989, A&A, 209, 126
Xiong, D. R., 1994, Acta Astron. Sinica 35, 1
Xiong, D. R. & Cheng, Q. L., 1992, A&A, 254, 362
Xiong, D. R., Cheng, Q. L. & Deng, L. 1995, submitted ApJ,

This article was processed by the author using Springer-Verlag LaTeX A&A style file *L-AA* version 3.